JACS
JOURNAL OF THE AMERICAN CHEMICAL SOCIETY
pubs.acs.org/JACS
Article

Pyridyl Radical-Induced Catalytic Reconstruction of Cyclic Sulfides

Yi-Peng Liu, Shi-Yu Guo,* Zhi-Yuan Ding, Yilitabaier Julaiti, Lian-Yue Wang,* Xiao-Feng Wu,* and Qing-An Chen*

Cite This: https://doi.org/10.1021/jacs.6c09452
Read Online

ABSTRACT: Ring-expansion editing offers a transformative strategy that could reshape the landscape of ring scaffold construction in synthetic chemistry. The introduction of three-dimensionality ring into flat aromatic systems could afford important semisaturated fused heterocycles, yet efficient method to access sulfur-containing semisaturated fused pyridines (SSFPs) remains scarce. Herein, we report a pyridyl radical-driven catalytic strategy for the direct two-carbon ring expansion of readily available cyclic thioethers, providing efficient access to synthetically challenging SSFPs. This transformation is enabled by synergistic dual photoredox cycles that orchestrate a cascade of radical cross-coupling, C(sp^3)−S bond cleavage, and intramolecular cyclization between commercial bromopyridines and cyclic sulfides. The protocol demonstrates broad functional-group tolerance and substrate generality. Gram-scale synthesis and extensive downstream derivatizations, including late-stage semisaturation of pharmaceutical cores, highlight its synthetic utility. Mechanistic studies support a stepwise radical process involving discrete pyridyl and carbon-centered radical intermediates. This method offers a step-economical and modular alternative to conventional de novo synthesis for the rapid construction of complex, drug-like heterocyclic architectures.

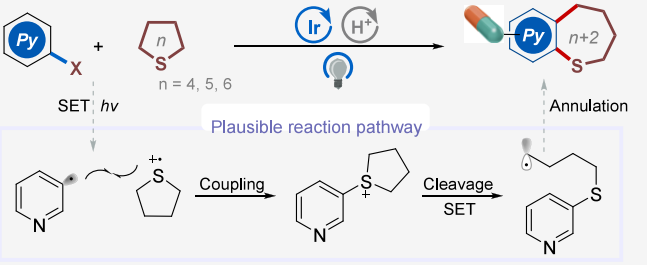

INTRODUCTION

Organic ring systems are foundational to pharmaceutical chemistry and materials science, with their two/three-dimensional (2D/3D) architecture directly governing physicochemical properties and application potential.[1−3] To overcome the limitations of predominantly planar drug candidates, the "escape from flatland" strategy[4−6] has become pivotal in drug discovery—introducing saturation into aromatic rings increases the Fsp^3 value and optimizes druggability (Figure 1a), making the precise synthesis of semisaturated fused ring scaffolds as a critical pursuit in organic synthesis.[7−13]

Pyridine, the most prevalent *N*-heterocyclic pharmacophore in FDA-approved drugs,[14] is a prime target for diverse functionalization,[15−25] particularly the construction of biologically active semisaturated fused pyridine 3D scaffolds (e.g., the core structures of Desloratadine, Blonanserin, and Cicletanine).[26−30] Meanwhile, sulfur-containing molecules account for ∼25% of active pharmaceutical ingredients (APIs),[14] as sulfur's unique electronic and structural properties enable precise modulation of biological activity[31]—exemplified by Dong's "carbonyl-to-sulfur swap"[32] and Koh's "oxygen−sulfur transmutation"[33] strategy. This renders sulfur-containing semisaturated fused pyridines (SSFPs) highly valuable in drug design due to their multiple activities, including multitargeted kinase inhibition, vitro antitumor and anti-influenza potency[34−37] (Figure 1a). Therefore, methods that permit the access to this class of SSFPs are highly sought after. However, current SSFPs synthesis relies primarily on de novo approaches, lacking efficient one-step catalytic methods. State-of-the-art strategies for semisaturated rings, including selective hydrogenation,[10,12,13] cycloaddition,[8,9,38] and radical cyclization,[39,40] face limitations of restricted precursor availability or transition metal catalyst deactivation in nitrogen- and sulfur-rich environments. Thus, a direct two-ring fusion strategy using commercial feedstocks is urgently needed to streamline access to these SSFPs scaffold (Figure 1a).

The ring enlargement of aromatic thiophenes was achieved by Glorius via insertion of bicyclo[1.1.0]butanes under photocatalysis.[41] However, ring expansion of saturated cyclic compounds is inherently challenging due to the low reactivity of σ-bonds. Methods for skeletal editing of cyclic amines and ethers have been reported,[42−46] while analogous transformations for cyclic thioethers—especially unstrained rings larger than four-membered—remain underdeveloped (Figure 1b). This gap stems from sulfur's intrinsic nucleophilicity, susceptibility to oxidation, and tendency to undergo undesired side reactions (e.g., ring opening). Classical ring expansion of thietanes relies on diazo compounds as carbene precursors under metal catalysis,[47] which is limited to small rings and

Received: May 8, 2026
Revised: June 6, 2026
Accepted: June 9, 2026

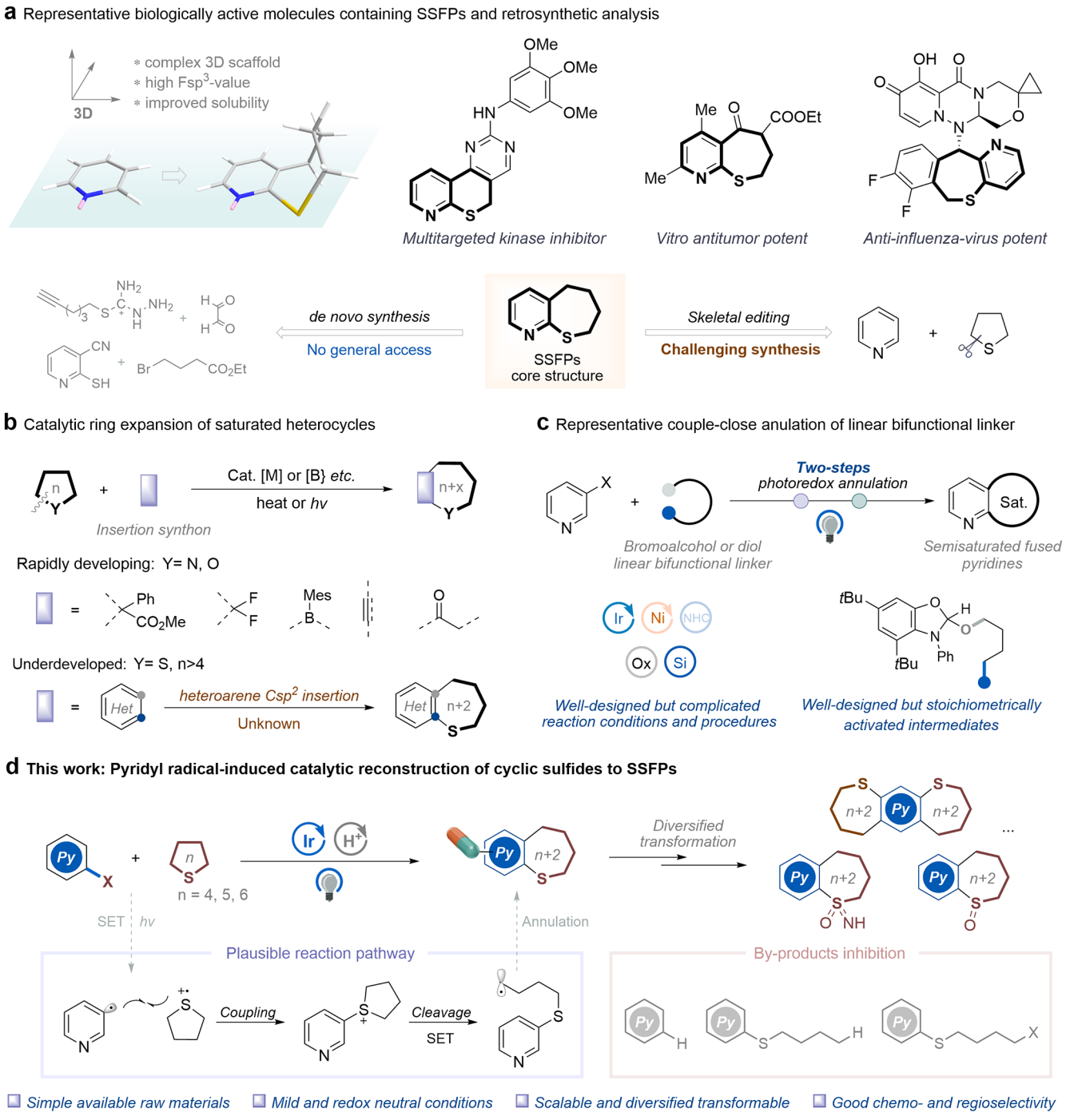

Figure 1. Catalytic reconstruction of cyclic sulfides for fused semisaturated heterocycles.

incompatible with larger cyclic thioethers. MacMillan's "couple-close" strategy enabled the synthesis of semisaturated fused pyridines via dual nickel/photoredox catalysis in two-steps.[11] During the submission of our manuscript,[48b] they reported an upgraded couple-close strategy via a cobalt-catalyzed dehydrogenative radical cyclization.[48a] These two works do not encompass the coupling of aryl halides with alkyl thiols and require well-designed linear diradical precursors, stoichiometric amounts of activator, and complex catalytic systems and reaction procedures, making it unsuitable for SSFPs (Figure 1c). In this context, cyclic thioethers are ideal C(sp^3)-rich precursors for SSFPs due to their commercial availability and high atom economy, yet their low reactivity typically necessitates preactivation to sulfonium salts or sulfoxides for downstream transformations.[49−51]

Addressing these challenges, we envisioned a pyridyl radical-induced reconstruction of cyclic thioethers to construct SSFPs. The key obstacle lies in integrating sequential C(sp^2)−S bond formation, C(sp^3)−S bond cleavage, and C(sp^3)−C(sp^2) ring closure in a single catalytic step. Herein, we report the realization of this concept by a photocatalytic ring-expansion reaction involving radical cross-coupling, C−S bond cleavage, and intramolecular cyclization between commercial bromopyridines and cyclic thioethers (Figure 1d). This transformation operates via two synergistic photoredox cycles: the first activates bromopyridine and cyclic thioether to form the

https://doi.org/10.1021/jacs.6c09452
J. Am. Chem. Soc. XXXX, XXX, XXX−XXX

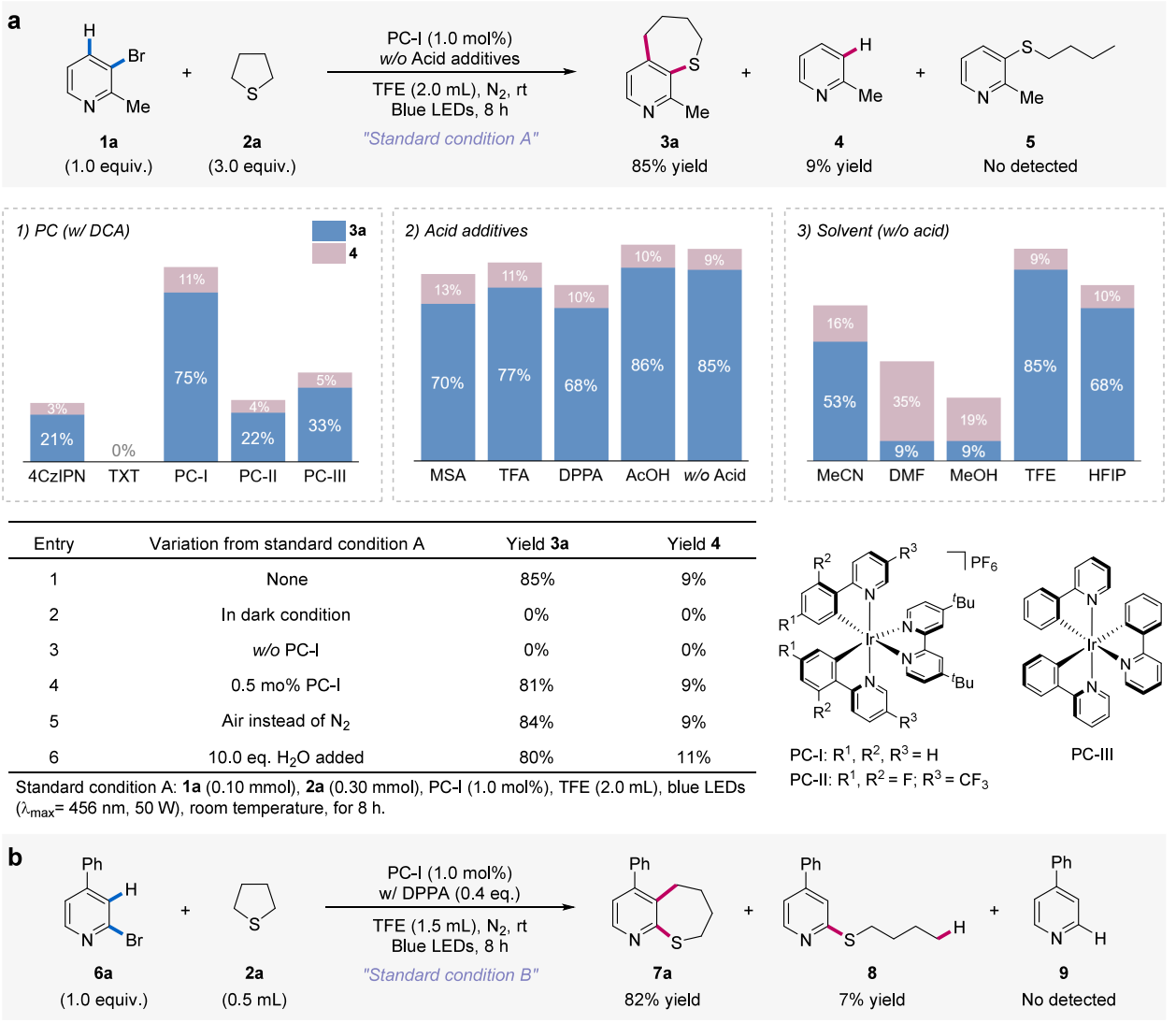

Entry	Variation from standard condition A	Yield **3a**	Yield **4**
1	None	85%	9%
2	In dark condition	0%	0%
3	*w/o* PC-I	0%	0%
4	0.5 mo% PC-I	81%	9%
5	Air instead of N_2	84%	9%
6	10.0 eq. H_2O added	80%	11%

Standard condition A: **1a** (0.10 mmol), **2a** (0.30 mmol), PC-I (1.0 mol%), TFE (2.0 mL), blue LEDs (λ_{max}= 456 nm, 50 W), room temperature, for 8 h.

PC-I: R^1, R^2, R^3 = H
PC-II: R^1, R^2 = F; R^3 = CF_3

Figure 2. Optimization of reaction conditions. (a) Standard condition A for 3-bromo-pyridines with thiophane. (b) Standard condition B for 2-bromo-pyridines with thiophane.

C(sp^2)−S bond, while the second mediates C(sp^3)−S bond cleavage and cyclization. This protocol enables access to synthetically challenging SSFPs, with broad utility highlighted by gram-scale synthesis, diverse sulfur-derived modifications, and late-stage semisaturation of complex bioactive molecules.

■ RESULTS AND DISCUSSION

To verify our hypothesis, the investigation was initiated with 2-methyl-3-bromopyridine (**1a**) and thiophane (**2a**) as the model reaction partners. After optimization, the ring-expansion product **3a** was obtained in 85% yield after reaction irradiated by blue LEDs for 8 h with Ir(dtbbpy)(ppy)$_2$PF$_6$ (PC-I) as the photocatalyst and trifluoroethanol (TFE) as the solvent without acid additives (Figure 2a). Meanwhile, the undesirable side reactions of dehalogenation (byproduct **4**) and ring-opening pyridylation (byproduct **5**) were effectively suppressed. Evaluation of the photocatalyst revealed that PC-I exhibited superior catalytic performance to other iridium photosensitizers or organophotocatalysts (chart 1). The photosensitizer thioxanthone (TXT) with high triplet energy directly prevented the model reaction from proceeding. Moreover, except for dichloroacetic acid (DCA), the use of other acid additives, such as methanesulfonic acid (MSA), trifluoroacetic acid (TFA), and diphenyl phosphate (DPPA), resulted in lower yields relative to those of acetic acid (AcOH) (chart 2). The acid is proposed to facilitate the protonation of the pyridine substrate, thereby promoting the initial single-electron transfer from the excited photocatalyst and the intramolecular cyclization step. Notably, the acid-free conditions also afforded the target product in a comparable yield of 85%. Several solvents were also screened and it was found that only strongly polar protic solvents could drive this ring-expansion conversion well (chart 3). Other common organic solvents adversely affected both the product yield and the chemoselectivity. The superior performance of TFE is likely attributed to its strong hydrogen-bond-donating ability and high polarity, which stabilize key radical intermediates. Based on the standard condition A, control experiments showed that blue LED irradiation and photocatalyst were essential to this reaction (Figure 2a, entries 2−3). Even at a reduced catalyst loading of 0.5 mol %, PC-I maintained a high yield of 81% for product **3a**, demonstrating its high catalytic efficiency (Figure 2a, entry 4). This optimized condition is tolerant to an air atmosphere and water (Figure 2a, entries 5−6). Additionally,

https://doi.org/10.1021/jacs.6c09452
J. Am. Chem. Soc. XXXX, XXX, XXX−XXX

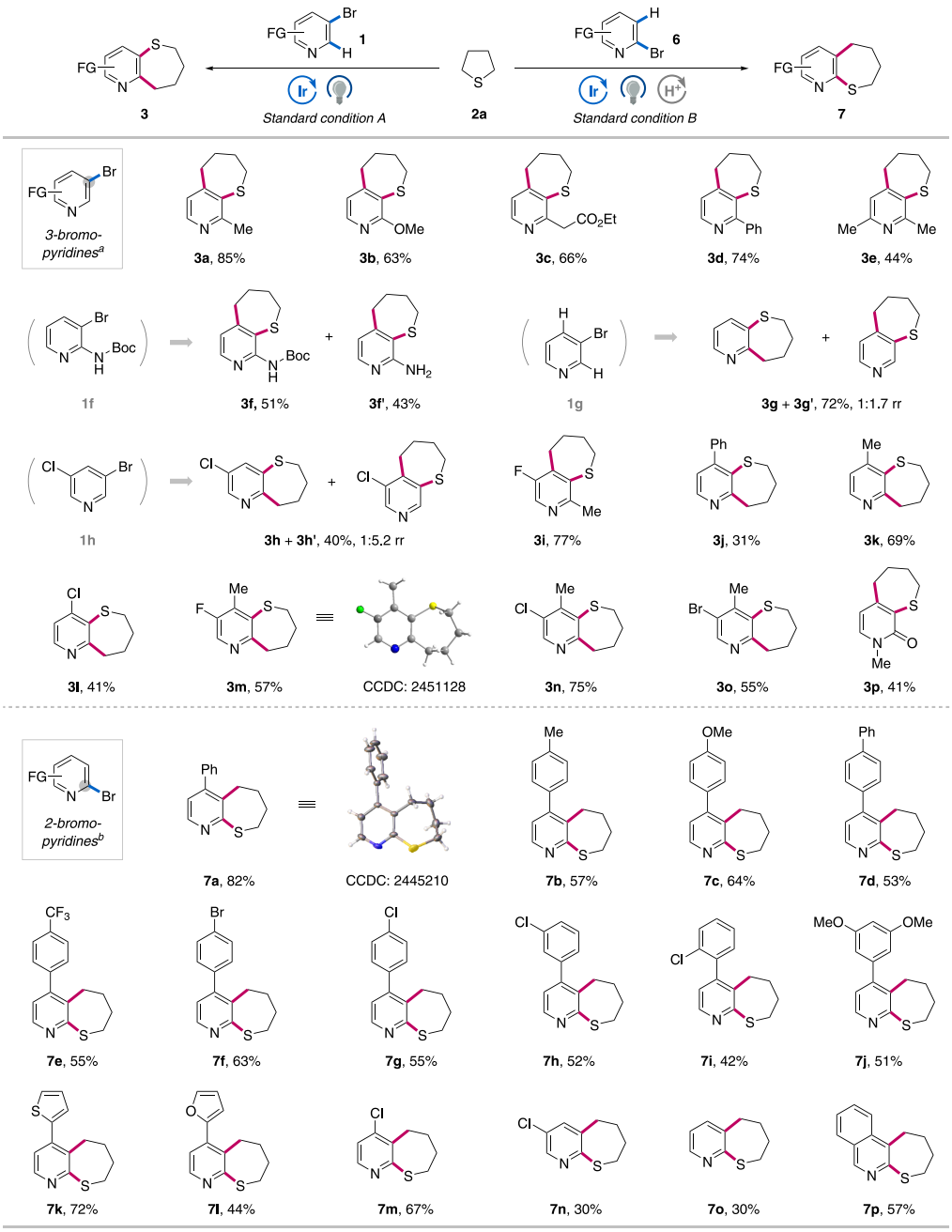

[a]Standard condition A: **1** (0.20 mmol), **2a** (0.60 mmol), PC-**I** (1.0 mol%), TFE (4.0 mL), blue LEDs (λ_{max}= 456 nm, 50 W), rt, 8 h.
[b]Standard condition B: **6** (0.20 mmol), **2a** (1.0 mL), PC-**I** (1.0 mol%), DPPA (0.4 eq.), TFE (3.0 mL), blue LEDs (λ_{max}= 456 nm, 50 W), rt, 8 h.

Figure 3. Substrate scope of pyridines.

by simply modifying the reaction conditions, 2-bromo-4-phenylpyridine **6a** was successfully inserted into thiophane, affording semisaturated product **7a** in 82% yield with only a 7% yield of ring-opening byproduct **8** (Figure 2b). Standard condition B for preparing **7a** involves adding 0.4 equiv of DPPA and 0.5 mL of **2a**. The different optimal acids likely originate from two key factors: varied reduction potentials of protonated bromopyridines and different cyclization reactivities of the regioisomers.

With the optimal conditions in hand, the substrate scope of this photocatalytic cyclic sulfides reconstruction reaction was explored. As shown in Figure 3, a series of commercially available 3-bromopyridines were first examined and provided the corresponding semisaturated products in moderate to good yields (**3a**−**3o**). Under the standard condition A, 3-bromopyridines with substitution at the C2 or C4 position could react smoothly with **2a** to generate desired 2,3,4,5-tetrahydrothiepino[2,3-*c*]pyridines (**3a**−**3f** and **3i**) and 6,7,8,9-tetrahydrothiepino[3,2-*b*]pyridines (**3j**−**3o**), respectively. 2,6-Dimethylbromopyridine was converted to the product with a moderate yield (**3e**, 44%), presumably due to impeded cyclization by the electron-rich pyridine ring. Reaction of substrate **1f** offered both the normal product (**3f**, 51% yield) and the *in situ* deprotection derivative (**3f′**, 43% yield). However, 3-bromopyridines bearing strong electron-withdrawing groups at the C2 and C4 positions were incompatible with this condition, presumably due to their inability to generate pyridyl radicals. The unsubstituted 3-bromopyridine

https://doi.org/10.1021/jacs.6c09452
J. Am. Chem. Soc. XXXX, XXX, XXX−XXX

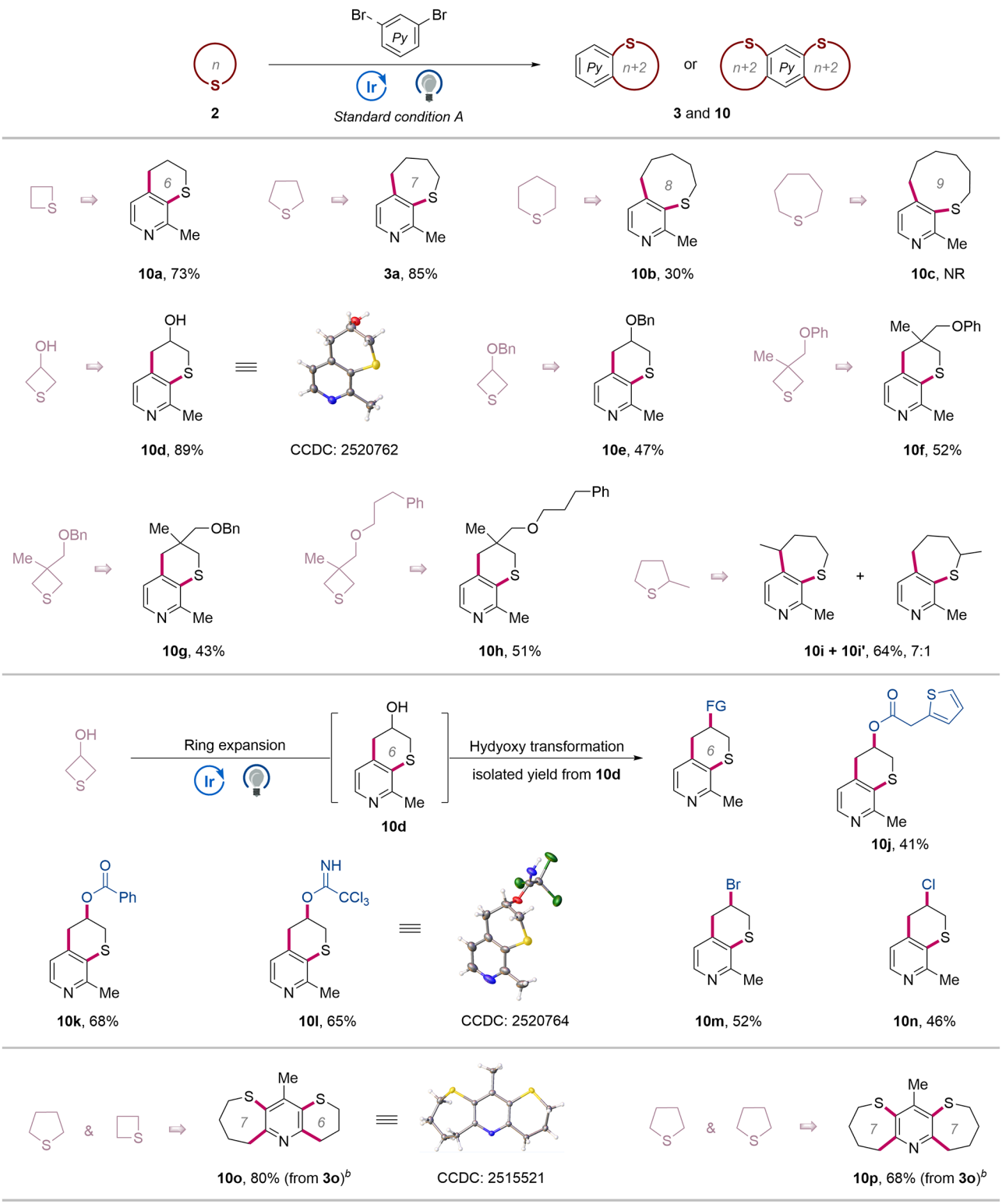

[a]Standard condition A: **1** (0.20 mmol), **2** (0.60 mmol), PC-I (1.0 mol%), TFE (4.0 mL), blue LEDs (λ_{max}= 456 nm, 50 W), rt, 8 h, isolated yields.
[b]Using **3o** as bromopyridine starting material.

Figure 4. Substrate scope of cyclic sulfides.

and 3-bromo-5-chloropyridine underwent both 2,3- and 2,4-annulation, affording two regioisomeric products (**3g** and **3g′**, 1:1.7 rr; **3h** and **3h′**, 1:5.2 rr). Notably, in the case of 3-bromopyridines containing an additional halogen substituent, reaction selectively took place at the C−Br bond, leaving C−Cl and C−F intact (**3i**, **3l**−**3n**). For the 3,5-dibromopyridine substrate, selective conversion of only one of the C−Br bonds was achieved through control of the reaction time (**3o**). The molecular structure of product **3m** was confirmed by X-ray analysis (CCDC 2451128). Moreover, the compatibility of bromopyridone substrate was also demonstrated with good regio- and chemoselectivity (**3p**).

https://doi.org/10.1021/jacs.6c09452
J. Am. Chem. Soc. XXXX, XXX, XXX−XXX

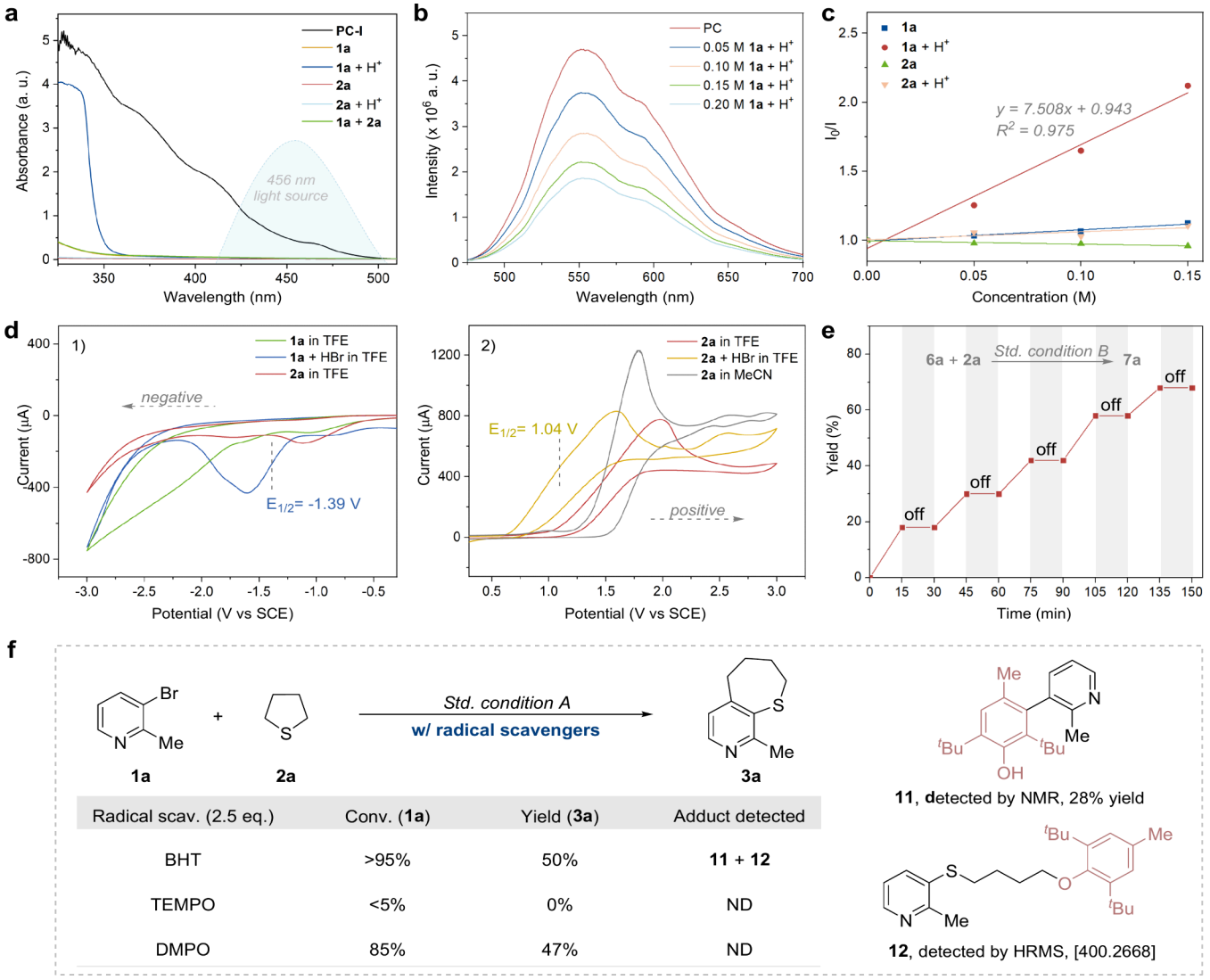

Radical scav. (2.5 eq.)	Conv. (**1a**)	Yield (**3a**)	Adduct detected
BHT	>95%	50%	**11** + **12**
TEMPO	<5%	0%	ND
DMPO	85%	47%	ND

Figure 5. Mechanistic studies. (a) UV−vis absorption spectroscopy. (b) Fluorescence quenching experiments. (c) Stern−Volmer plots of PC-I with different quenchers. (d) Cyclic voltammetry analysis of substrates. (e) Light on/off experiments. (f) Radical trapping experiments.

Encouraged by the results above, we sought to examine the scope of 2-bromopyridine derivatives under standard condition B. In contrast to the 3-bromopyridines, the 2-bromopyridines underwent exclusive 2,3-annulation, albeit with greater challenge due to their lower reactivity at C3 position. As shown in Figure 3, a wide range of C4 aryl-substituted bromopyridines demonstrated good tolerance in this method and gave synthetically useful yields (**7a**−**7l**). Both the electronic nature (**7b**−**7f**) and the position (**7g**−**7j**) of the substituents on the phenyl showed minimal impact on the reaction outcome. Heteroaryl substituents, including thiophene- and furan-substituted pyridines, afforded the corresponding products in 72% (**7k**) and 44% (**7l**) yields, respectively. And these two target molecules further increase the heterocyclic diversity of product. Chloro substituents at C4 and C5 of 2-bromopyridine were also tolerated, delivering corresponding products with C−Cl bond preservation for further synthetic elaboration (**7m** and **7n**). The reaction of unsubstituted 2-bromopyridine with thiophane proceeded inefficiently, producing the desired product **7o** in 30% yield alongside substantial ring-opening byproducts. Notably, this conversion was successfully extended to bromoisoquinoline, generating semisaturated fused tricyclic compound **7p** in 57% yield. Several additional (hetero)aryl bromides were evaluated under the standard conditions, including brominated quinoline, isoquinoline, pyrrolo-indole, pyrimidine, pyrazine and bromobenzene, yet all displayed low reactivity to afford merely trace product or no conversion. Further evaluation on 4-bromopyridine delivered low efficiency and selectivity, likely due to reduced electrophilicity of the 4-pyridyl radical as well as poor reactivity for intramolecular cyclization at C3 position (Figure 1 in Supporting Information).

Subsequently, we turned our attention to the cyclic sulfide substrates (Figure 4). Using the strained thietane, the corresponding product obtained from this ring expansion was 6,6-fused semisaturated pyridine (**10a**, 73% yield). As demonstrated by the results of model reaction, thiophane as a low-strain cyclic thioether, was proved to be an excellent ring-expansion precursor under our reaction conditions (**3a**, 85% yield). Besides, we were pleased to find that unstrained 6-membered cyclic thioether also performed feasibly, delivering the 6,8-fused bicyclic compound **10b** in synthetically useful yield. The larger, seven-membered cyclic thioether was also explored, but no desired product was observed (**10c**). This

https://doi.org/10.1021/jacs.6c09452
J. Am. Chem. Soc. XXXX, XXX, XXX−XXX

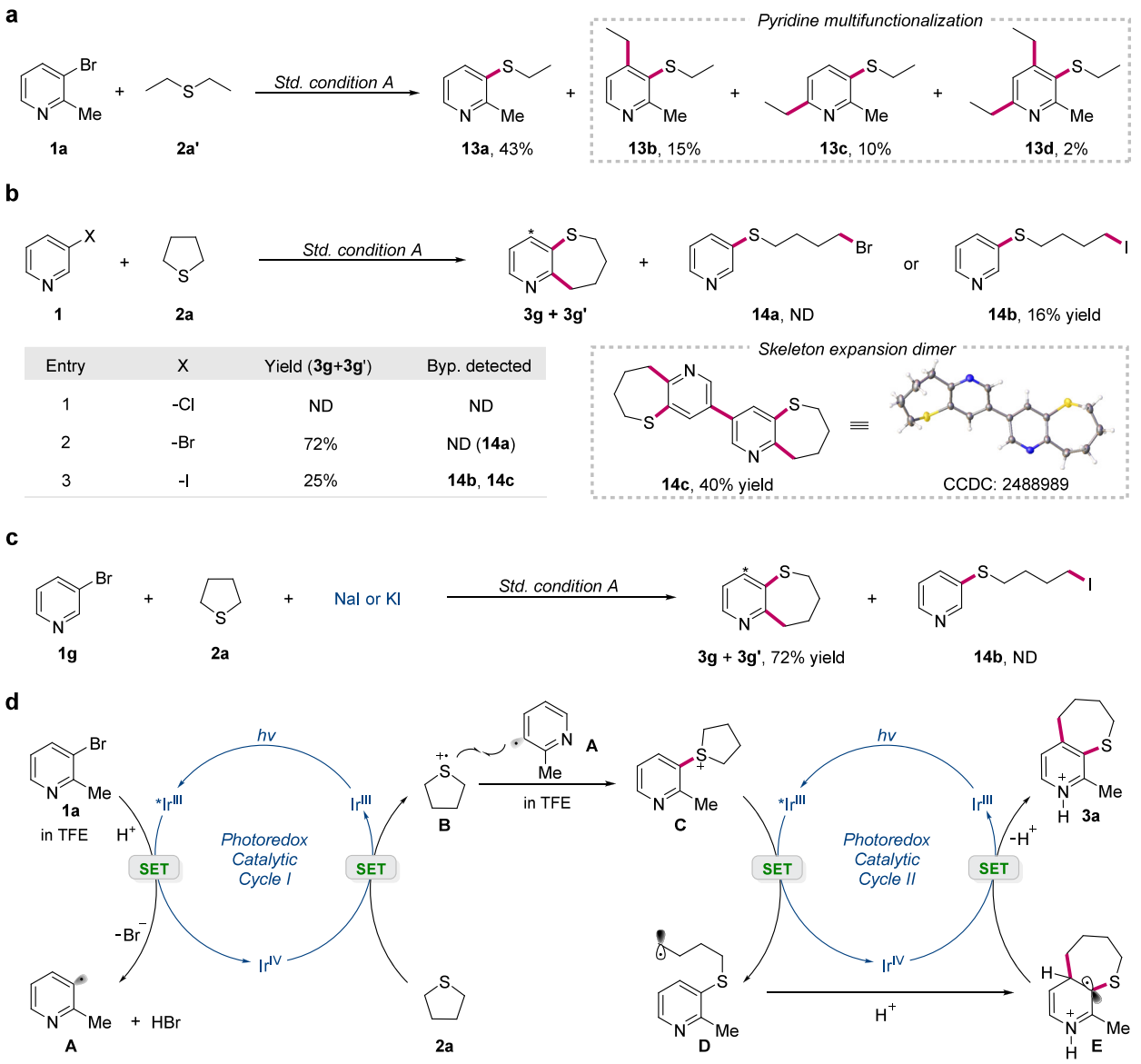

Figure 6. Control experiments and proposed mechanism. (a) Pyridyl radical-mediated cleavage of C−S bonds in linear thioethers. (b) Study on the chemoselective behavior of different halopyridines. (c) Competitive experiments. (d) Plausible mechanism.

observation might support that the ring strain of the sulfonium intermediate serves as a crucial driving force for the reaction. The lower strain in the 6- and 7-membered cyclic thioether intermediates accounts for their poor reactivity. Thietanes with common functionalities such as hydroxy (**10d**), benzyloxy (**10e** and **10g**), phenoxy (**10f**) and alkoxy (**10h**) could be reconstructed under standard condition, exhibiting good functional group tolerance. The reaction of 2-methyltetrahydrothiophene gave ring-expansion product **10i** and **10i′** in 64% total yield with a 7:1 ratio of regioisomers, which implies a radical cyclization pathway for the reaction. Based on compound **10d**, further transformation of the hydroxy group afforded a series of thioether-fused pyridine products bearing diverse substituents (Section 7 in Supporting Information), including ester (**10j**), OBz (**10k**), imidate (**10l**), and halogen groups (**10m**−**10n**). Interestingly, 3-bromo semisaturated fused pyridine **3o** prepared by this method can be further converted into 7,6,6- and 7,6,7-fused tricyclic products **10o** and **10p**, which constitute challenging scaffolds absent from existing literature.

To elucidate the mechanism of this skeletal expansion fusion reaction, a series of mechanistic studies and intermediates exploration were conducted (Figures 5 and 6). UV/vis absorption experiments indicated that the photocatalyst was the sole light-absorbing species within the wavelength of light irradiation source (Figure 5a). And this observation also precludes the possibility of substrate aggregation forming light-absorbing EDA complexes. Fluorescence quenching experiments and the Stern−Volmer analysis showcased that the excited-state PC-I* was quenched by bromopyridine **1a** rather than thioether **2a** (Figures 5b and 5c). The addition of protic acid could significantly enhance the quenching of the photocatalyst by the pyridine substrate, which is consistent with our experimental observations above. To further elucidate the electron transfer behavior of the substrates, cyclic voltammetry experiments were conducted (Figure 5d and Section 8.3 in Supporting Information). As shown in Figure 5d, a reductive peak of **1a** was detected at −1.39 V when mixed with HBr in TFE (eq 1, blue line). However, in the absence of acid, the reduction peak of **1a** disappeared (eq 1, green line).

https://doi.org/10.1021/jacs.6c09452
J. Am. Chem. Soc. XXXX, XXX, XXX−XXX

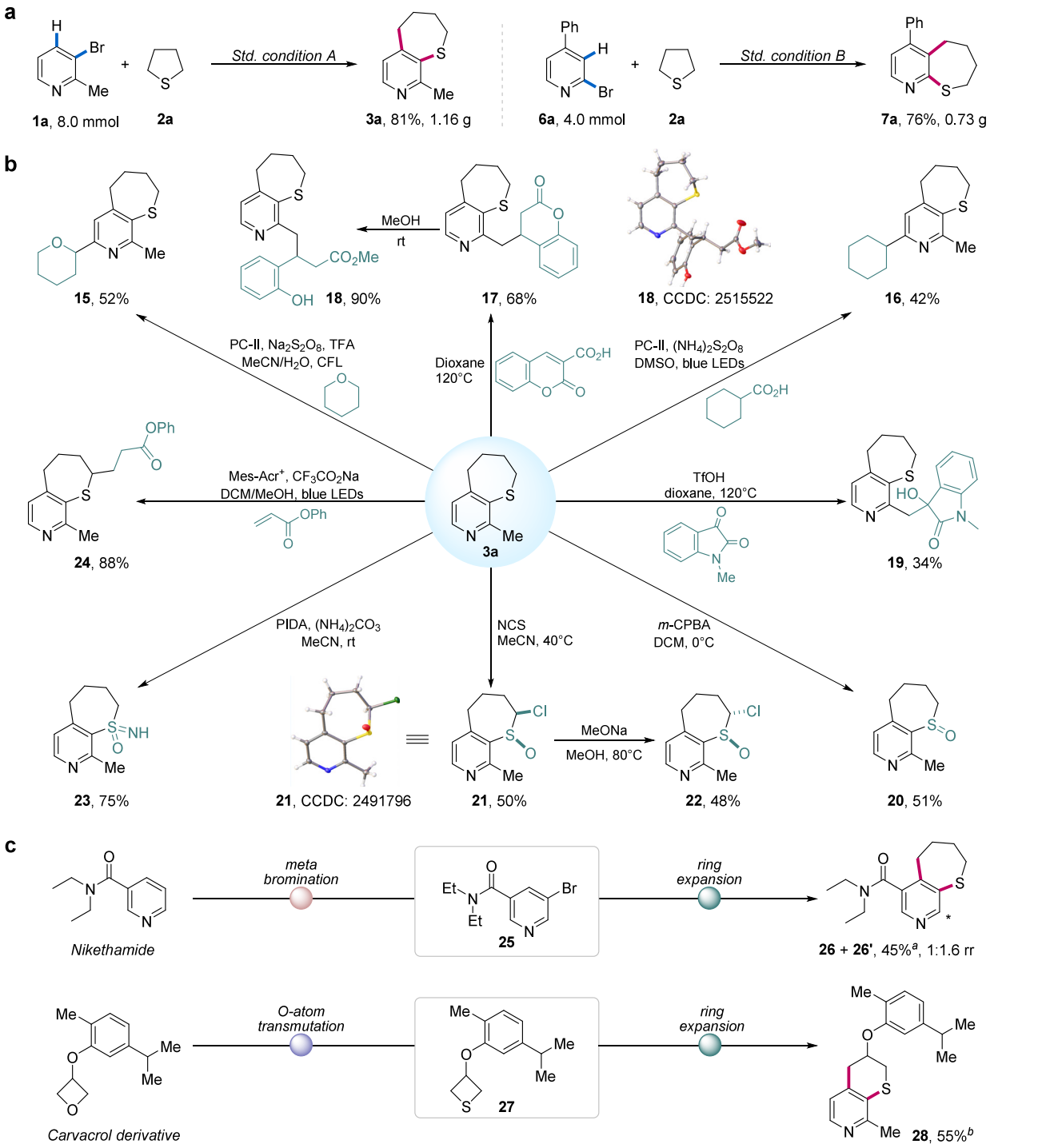

Figure 7. Synthetic applications. (a) Gram-scale synthesis. (b) Synthetic derivatization. (c) Late-stage modification of drug variants. [a]Isolated yield from intermediate **25**. [b]Isolated yield from intermediate **27**.

No reduction peak was observed for thiophane **2a** in this condition (eq 1, red line). These results reveal that bromopyridine **1a** is feasibly reduced via SET pathway by the PC-I*. Further positive scanning found that thiophane **2a** could be oxidized at 1.58 V in TFE (eq 2, red line), whereas delivered a lower oxidation potential upon the addition of acid (eq 2, yellow line and Figure 11 in Supporting Information), which implied that the thiophane **2a** might serve as a reductant in this reaction. Moreover, light on/off experiments demonstrated that this reaction ceased in the dark and effectively restored upon light irradiation, thus demonstrating the crucial role of light irradiation and excluding a long radical chain process (Figure 5e). Radical trapping experiments were then conducted and the reaction was suppressed in the presence of radical inhibitor 2,2,6,6-tetramethyl-1-piperidinyloxy (TEMPO), butylated hydroxytoluene (BHT), or 5,5-dimethyl-1-pyrroline *N*-oxide (DMPO), which hints the radical nature of this ring expansion process (Figure 5f). Trapping of two radical adduct intermediates **11** and **12** suggests the pyridyl

https://doi.org/10.1021/jacs.6c09452
J. Am. Chem. Soc. XXXX, XXX, XXX−XXX

radical and the ring-opening carbon radical as the likely active species in this transformation.

To further probe the mechanism of C(sp^3)−S bond cleavage and subsequent C(sp^2)−S bond formation, control experiments were conducted to verify our proposed hypothesis (Figure 6). First, when the linear thioether **2a′** was used in place of cyclic thioether **2a**, no ring-expansion product was formed (Figure 6a). Instead, an *ipso* sulfenylation product **13a** was obtained in 43% yield. Notably, several pyridyl thioether/alkylated multifunctionalization products (**13b**−**13d**) were also detected. We then examined the chemoselectivity of various 3-halopyridines, such as chloro-, bromo- and iodopyridines under standard condition A. The 3-chloropyridine substrate remained unreactive, yielding no product. The 3-bromopyridine exclusively formed the previously observed ring-expansion products (**3g** and **3g′**), with no ring-opening bromination product (**14a**). Interestingly, the reaction of 3-iodopyridine exhibited diverse chemoselectivity, yielding not only the target ring-expansion product but also ring-opening iodination adduct (**14b**) and an unexpected dimerized ring-expansion derivative (**14c**). We hypothesized that the iodide anion exhibits stronger nucleophilicity than bromide in TFE, which may promote C−S bond cleavage of the in situ formed pyridinium sulfonium to deliver byproduct **14b**. But the formation mechanism of the dimeric byproduct **14c** remains unclear. Moreover, when exogenous iodide was added to the reaction of 3-bromopyridine, the original transformation remained unaffected, and no ring-opening iodination byproduct **14b** was detected (Figure 6c), likely attributed to the solvent cage effect.[52,53]

In light of the above results, a proposed mechanism including two photoredox catalytic cycles is described in detail (Figure 6d). Specifically, photoexcitation of photocatalyst Ir^{III} generates its excited state $*Ir^{III}$. Oxidative quenching of $*Ir^{III}$ ($*E_{1/2}^{ox}$ = −1.54 V vs SCE in TFE)[21,54,55] by bromopyridine **1a** via single-electron transfer (SET) provides oxidative Ir^{IV} species, a pyridyl radical **A**, and an equivalent of halide anion. The subsequent SET from thioether **2a** to the Ir^{IV} species ($E_{1/2}^{red}$ = 0.98 V vs SCE in TFE)[21,54,55] affords sulfur radical cation **B** and regenerates the Ir^{III} photocatalyst. Sulfonium salt intermediate **C** is formed through rapid coupling of the two radical species **A** and **B**. Next, within the second photoredox cycle, the sulfonium salt **C** undergoes SET with photoexcited $*Ir^{III}$, yielding the alkyl radical intermediate **D** and Ir^{IV} species via the cleavage of the C(sp^3)−S bond.[51,56] The resulting radical **D** then participates in an intramolecular addition to form the radical cation **E**. Finally, oxidation and deprotonation of **E** by the Ir^{IV} species afford the target SSFP **3a**, concurrently regenerating the ground state Ir^{III} photocatalyst.

Afterward, synthetic applications of the SSFPs scaffold were investigated (Figure 7 and Section 7 in Supporting Information). Gram-scale synthesis was achieved by reactions between bromopyridines and thiophane **2a**, affording semisaturated fused pyridines **3a** and **7a** in 81% (1.16 g) and 76% (0.73 g) yields, respectively (Figure 7a). Starting from compound **3a**, pyridine alkylation products (**15** and **16**) were obtained in moderate yields through the photoinduced Minisci pathway (Figure 7b).[57,58] The selective sp^3 C−H functionalization on the methyl group of pyridines allowed for facile synthesis of biologically important azaarene-substituted 3,4-dihydro-coumarin (**17**)[59] and 3-hydroxy-2-oxindole (**19**).[60] Nucleophilic attack by methanol on compound **17** resulted in lactone ring-opening, affording product **18** in 90% yield. Selective oxidation of **3a** produced sulfoxide (**20**−**22**) and sulfoximine (**23**), demonstrating the versatility of sulfonyl transformations. Notably, when *N*-chlorosuccinimide (NCS) was employed as the oxidant, substrate **3a** was directly converted to the α-chlorinated sulfoxide product **21**[61,62] and its relative configuration was further confirmed by single-crystal X-ray crystallography (CCDC 2491796). Furthermore, the product **21** underwent an epimerization in the presence of methanol/sodium methoxide to yield its diastereoisomer **22**. Selective C−H activation of *S*-α-C(sp^3)−H offered desired alkylated products (**24**) in 88% yield through photoredox catalysis.[63]

To enable rapid modification while circumventing de novo synthesis, we applied our method to achieve the late-stage semisaturation of various pharmaceutically relevant moieties (Figure 7c). Nikethamide was successfully converted into the corresponding semisaturated fused product **26** through *meta*-bromination[24] and our ring expansion transformation. The oxetane scaffold decorated with carvacrol underwent O atom transmutation to afford the corresponding thietane,[33] which then participated in our reconstruction reaction with bromopyridine to yield the target product **28**.

CONCLUSION

In conclusion, we have developed a photocatalytic cascade reaction that enables the direct reconstruction of unstrained cyclic thioethers into valuable sulfur-containing fused semisaturated pyridine scaffolds. This strategy successfully addresses the challenge of skeletal editing for cyclic sulfides by leveraging a pyridyl radical-mediated sequential C−S bond formation and cleavage processes. The method operates under mild and redox neutral conditions using simple feedstocks, exhibits excellent functional group tolerance, and provides access to a diverse array of previously difficult-to-access bicyclic and tricyclic architectures. Mechanistic investigations support a mechanism involving two synergistic photoredox catalytic cycles. The SSFPs core scaffold serves as a versatile platform for diverse postsynthetic modifications, providing direct access to the late-stage semisaturation of complex bioactive molecules. Given the high prevalence of both pyridine and sulfur motifs in pharmaceuticals, we anticipate this efficient and step-economical protocol will find immediate utility in medicinal chemistry and drug discovery for the rapid synthesis of high-value three-dimensional heterocycles.

ASSOCIATED CONTENT

Supporting Information

The Supporting Information is available free of charge at https://pubs.acs.org/doi/10.1021/jacs.6c09452.

Experimental procedures, characterization data, and NMR spectra (PDF)

Accession Codes

Deposition Numbers 2445210, 2451128, 2488989, 2491796, 2515521−2515522, 2520762, and 2520764 contain the supplementary crystallographic data for this paper. These data can be obtained free of charge via the joint Cambridge Crystallographic Data Centre (CCDC) and Fachinformationszentrum Karlsruhe Access Structures service.

https://doi.org/10.1021/jacs.6c09452
J. Am. Chem. Soc. XXXX, XXX, XXX−XXX

AUTHOR INFORMATION

Corresponding Authors

Shi-Yu Guo − *Dalian Institute of Chemical Physics, Chinese Academy of Sciences, Dalian 116023, China; University of Chinese Academy of Sciences, Beijing 100049, China*; Email: carlosguo10@dicp.ac.cn

Lian-Yue Wang − *Liaoning Normal University, Dalian 116029, China*; orcid.org/0000-0002-0954-6857; Email: lianyuewang@lnnu.edu.cn

Xiao-Feng Wu − *Dalian Institute of Chemical Physics, Chinese Academy of Sciences, Dalian 116023, China; Leibniz-Institut für Katalyse e.V., Rostock 18059, Germany; University of Chinese Academy of Sciences, Beijing 100049, China*; orcid.org/0000-0001-6622-3328; Email: xwu2020@dicp.ac.cn

Qing-An Chen − *Dalian Institute of Chemical Physics, Chinese Academy of Sciences, Dalian 116023, China; University of Chinese Academy of Sciences, Beijing 100049, China*; orcid.org/0000-0002-9129-2656; Email: qachen@dicp.ac.cn

Authors

Yi-Peng Liu − *Dalian Institute of Chemical Physics, Chinese Academy of Sciences, Dalian 116023, China; Leibniz-Institut für Katalyse e.V., Rostock 18059, Germany*

Zhi-Yuan Ding − *Dalian Institute of Chemical Physics, Chinese Academy of Sciences, Dalian 116023, China; University of Chinese Academy of Sciences, Beijing 100049, China*

Yilitabaier Julaiti − *Dalian Institute of Chemical Physics, Chinese Academy of Sciences, Dalian 116023, China; University of Chinese Academy of Sciences, Beijing 100049, China*

Complete contact information is available at: https://pubs.acs.org/10.1021/jacs.6c09452

Notes

The authors declare no competing financial interest.

ACKNOWLEDGMENTS

We acknowledge financial support from the Dalian Institute of Chemical Physics (DICP I202423) and the National Natural Science Foundation of China (22301299).

REFERENCES

(1) Aldeghi, M.; Malhotra, S.; Selwood, D. L.; Chan, A. W. Two- and three-dimensional rings in drugs. *Chem. Biol. Drug. Des.* **2014**, *83*, 450−461.

(2) Taylor, R. D.; MacCoss, M.; Lawson, A. D. Rings in drugs. *J. Med. Chem.* **2014**, *57*, 5845−5859.

(3) Chen, Y.; Rosenkranz, C.; Hirte, S.; Kirchmair, J. Ring systems in natural products: structural diversity, physicochemical properties, and coverage by synthetic compounds. *Nat. Prod. Rep.* **2022**, *39*, 1544−1556.

(4) Lovering, F.; Bikker, J.; Humblet, C. Escape from flatland: increasing saturation as an approach to improving clinical success. *J. Med. Chem.* **2009**, *52*, 6752−6756.

(5) Cox, B.; Zdorichenko, V.; Cox, P. B.; Booker-Milburn, K. I.; Paumier, R.; Elliott, L. D.; Robertson-Ralph, M.; Bloomfield, G. Escaping from flatland: substituted bridged pyrrolidine fragments with inherent three-dimensional character. *ACS Med. Chem. Lett.* **2020**, *11*, 1185−1190.

(6) Morley, A. D.; Pugliese, A.; Birchall, K.; Bower, J.; Brennan, P.; Brown, N.; Chapman, T.; Drysdale, M.; Gilbert, I. H.; Hoelder, S.; Jordan, A.; Ley, S. V.; Merritt, A.; Miller, D.; Swarbrick, M. E.; Wyatt, P. G. Fragment-based hit identification: thinking in 3D. *Drug Discovery Today* **2013**, *18*, 1221−1227.

(7) Twigg, D. G.; Kondo, N.; Mitchell, S. L.; Galloway, W. R. J. D.; Sore, H. F.; Madin, A.; Spring, D. R. Partially saturated bicyclic heteroaromatics as an sp^3-enriched fragment collection. *Angew. Chem., Int. Ed.* **2016**, *55*, 12479−12483.

(8) Ma, J.; Chen, S.; Bellotti, P.; Guo, R.; Schäfer, F.; Heusler, A.; Zhang, X.; Daniliuc, C.; Brown, M. K.; Houk, K. N.; Glorius, F. Photochemical intermolecular dearomative cycloaddition of bicyclic azaarenes with alkenes. *Science* **2021**, *371*, 1338−1345.

(9) Ma, J.; Chen, S.; Bellotti, P.; Wagener, T.; Daniliuc, C.; Houk, K. N.; Glorius, F. Facile access to fused 2D/3D rings via intermolecular cascade dearomative [2 + 2] cycloaddition/rearrangement reactions of quinolines with alkenes. *Nat. Catal.* **2022**, *5*, 405−413.

(10) Liu, D. H.; Pfluger, P. M.; Outlaw, A.; Luckemeier, L.; Zhang, F.; Regan, C.; Rashidi Nodeh, H.; Cernak, T.; Ma, J.; Glorius, F. Late-stage saturation of drug molecules. *J. Am. Chem. Soc.* **2024**, *146*, 11866−11875.

(11) Long, A.; Oswood, C. J.; Kelly, C. B.; Bryan, M. C.; MacMillan, D. W. C. Couple-close construction of polycyclic rings from diradicals. *Nature* **2024**, *628*, 326−332.

(12) Hu, C.; Cai, C. Y.; Barta, E. S.; Merchant, R. R.; Matsuura, B. S.; Chen, S. J.; Chen, S.; Qin, T. Ligand-controlled regioselective dearomative vicinal and conjugate hydroboration of quinolines. *J. Am. Chem. Soc.* **2025**, *147*, 11906−11914.

(13) Pierau, M.; Karrasch, M. J.; Hartmann, P.; Daniliuc, C. G.; Hamza, A.; Glorius, F. Direct access to chiral nitrogen-rich (semi-)saturated heterocycles. *Chem.* **2026**, *12*, 102817.

(14) Marshall, C. M.; Federice, J. G.; Bell, C. N.; Cox, P. B.; Njardarson, J. T. An update on the nitrogen heterocycle compositions and properties of U.S. FDA-approved pharmaceuticals (2013−2023). *J. Med. Chem.* **2024**, *67*, 11622−11655.

(15) Guo, S.-Y.; Yang, F.; Song, T.-T.; Guan, Y.-Q.; Min, X.-T.; Ji, D.-W.; Hu, Y.-C.; Chen, Q.-A. Photo-induced catalytic halopyridylation of alkenes. *Nat. Commun.* **2021**, *12*, 6538.

(16) Boyle, B. T.; Levy, J. N.; de Lescure, L.; Paton, R. S.; McNally, A. Halogenation of the 3-position of pyridines through Zincke imine intermediates. *Science* **2022**, *378*, 773−779.

(17) Cao, H.; Cheng, Q.; Studer, A. Radical and ionic *meta*-C−H functionalization of pyridines, quinolines, and isoquinolines. *Science* **2022**, *378*, 779−785.

(18) Le Saux, E.; Georgiou, E.; Dmitriev, I. A.; Hartley, W. C.; Melchiorre, P. Photochemical organocatalytic functionalization of pyridines via pyridinyl radicals. *J. Am. Chem. Soc.* **2023**, *145*, 47−52.

(19) Lee, W.; Koo, Y.; Jung, H.; Chang, S.; Hong, S. Energy-transfer-induced [3 + 2] cycloadditions of *N-N* pyridinium ylides. *Nat. Chem.* **2023**, *15*, 1091−1099.

(20) Boudry, E.; Bourdreux, F.; Marrot, J.; Moreau, X.; Ghiazza, C. Dearomatization of pyridines: photochemical skeletal enlargement for the synthesis of 1,2-diazepines. *J. Am. Chem. Soc.* **2024**, *146*, 2845−2854.

(21) Guo, S.-Y.; Liu, Y.-P.; Huang, J.-S.; He, L.-B.; He, G.-C.; Ji, D.-W.; Wan, B.; Chen, Q.-A. Visible light-induced chemoselective 1,2-diheteroarylation of alkenes. *Nat. Commun.* **2024**, *15*, 6102.

(22) Siddiqi, Z.; Bingham, T. W.; Shimakawa, T.; Hesp, K. D.; Shavnya, A.; Sarlah, D. Oxidative dearomatization of pyridines. *J. Am. Chem. Soc.* **2024**, *146*, 2358−2363.

(23) Chen, Z.-H.; Liu, L.; Wang, Y.-B.; Luo, H.; Tang, Z.-L.; Zhou, X.-Y.; Wang, X.-C. Methylation and alkylation of pyridines at the *meta* position using aldehydes or aldehyde surrogates. *J. Am. Chem. Soc.* **2025**, *147*, 36882−36889.

(24) Li, C.; Li, X.; Li, J.; Wang, Z.; Ouyang, D.; Jiao, N.; Song, S. Direct regioselective C-3 halogenation of pyridines. *Nat. Synth.* **2026**, *5*, 36−45.

(25) Zhang, J.; Wu, G.; Zhao, Y.; Liu, X.; Zhu, H.; Studer, A.; Qi, X.; Cheng, Q. Spin-density-controlled radical coupling for *meta*-selective C−H halogenation of pyridines. *Nat. Synth.* **2026**, *5*, 27−35.
(26) Geha, R. S.; Meltzer, E. O. Desloratadine: a new, nonsedating, oral antihistamine. *J. Allergy Clin. Immunol.* **2001**, *107*, 751−762.
(27) Fedorova, O. V.; Talan, M. I.; Agalakova, N. I.; Droy-Lefaix, M.-T.; Lakatta, E. G.; Bagrov, A. Y. Myocardial PKC β2 and the sensitivity of Na/K-ATPase to marinobufagenin are reduced by cicletanine in dahl hypertension. *Hypertension* **2003**, *41*, 505−511.
(28) Deeks, E. D.; Keating, G. M. Blonanserin. *CNS Drugs* **2010**, *24*, 65−84.
(29) Ueno, T.; Matsuoka, E.; Asada, N.; Yamamoto, S.; Kanegawa, N.; Ito, M.; Ito, H.; Moechars, D.; Rombouts, F. J. R.; Gijsen, H. J. M.; Kusakabe, K.-i. Discovery of extremely selective fused pyridine-derived β-site amyloid precursor protein-cleaving enzyme (BACE1) inhibitors with high in vivo efficacy through 10s loop interactions. *J. Med. Chem.* **2021**, *64*, 14165−14174.
(30) Luo, G.; Chen, L.; Conway, C. M.; Denton, R.; Keavy, D.; Gulianello, M.; Huang, Y.; Kostich, W.; Lentz, K. A.; Mercer, S. E.; Schartman, R.; Signor, L.; Browning, M.; Macor, J. E.; Dubowchik, G. M. Discovery of BMS-846372, a potent and orally active human CGRP receptor antagonist for the treatment of migraine. *ACS Med. Chem. Lett.* **2012**, *3*, 337−341.
(31) Feng, M. H.; Tang, B. Q.; Liang, S. H.; Jiang, X. F. Sulfur containing scaffolds in drugs: synthesis and application in medicinal chemistry. *Curr. Top. Med. Chem.* **2016**, *16*, 1200−1216.
(32) Zhang, Z.; Dong, G. Carbonyl-to-sulfur swap enabled by sequential double carbon-carbon bond activation. *Science* **2025**, *388*, 1436−1440.
(33) Zhang, Y. Q.; Li, S. H.; Zhang, X.; Koh, M. J. Photocatalytic oxygen-atom transmutation of oxetanes. *Nature* **2025**, *647*, 906−912.
(34) Tagawa, H.; Kubo, S.; Ishikawa, F. Nonsteroidal antiinflammatory agents. IV. Syntheses of pyridobenzoxepin, pyridobenzothiepin and their acetic acid derivatives. *Chem. Pharm. Bull.* **1981**, *29*, 3515−3521.
(35) Kumazawa, T.; Harakawa, H.; Obase, H.; Oiji, Y.; Tanaka, H.; Shuto, K.; Ishii, A.; Oka, T.; Nakamizo, N. Synthesis and antiulcer activity of 5,11-dihydro[1]benzoxepino[3,4-b]pyridines. *J. Med. Chem.* **1988**, *31*, 779−785.
(36) Waly, M. A.; Elhawary, I. I.; Elgogary, T. M. Utilization of nicotinonitrile-2-thiol in the synthesis of new thiepino[2,3-b]pyridine derivative as an in vitro novel antitumor potent. *Med. Chem. Res.* **2013**, *22*, 1674−1678.
(37) Salerno, S.; Barresi, E.; Garcia-Argaez, A. N.; Taliani, S.; Simorini, F.; Amendola, G.; Tomassi, S.; Cosconati, S.; Novellino, E.; Da Settimo, F.; Marini, A. M.; Dalla Via, L. Discovery of pyrido[3′,2′:5,6]thiopyrano[4,3-d]pyrimidine-based antiproliferative multikinase inhibitors. *ACS Med. Chem. Lett.* **2019**, *10*, 457−462.
(38) Poplata, S.; Tröster, A.; Zou, Y.-Q.; Bach, T. Recent advances in the synthesis of cyclobutanes by olefin [2 + 2] photocycloaddition reactions. *Chem. Rev.* **2016**, *116*, 9748−9815.
(39) Bordi, S.; Starr, J. T. Hydropyridylation of olefins by intramolecular Minisci reaction. *Org. Lett.* **2017**, *19*, 2290−2293.
(40) Maust, M. C.; Hendy, C. M.; Jui, N. T.; Blakey, S. B. Switchable regioselective 6-endo or 5-exo radical cyclization via photoredox catalysis. *J. Am. Chem. Soc.* **2022**, *144*, 3776−3781.
(41) Wang, H.; Shao, H.; Das, A.; Dutta, S.; Chan, H. T.; Daniliuc, C.; Houk, K. N.; Glorius, F. Dearomative ring expansion of thiophenes by bicyclobutane insertion. *Science* **2023**, *381*, 75−81.
(42) Lyu, H.; Kevlishvili, I.; Yu, X.; Liu, P.; Dong, G. Boron insertion into alkyl ether bonds via zinc/nickel tandem catalysis. *Science* **2021**, *372*, 175−182.
(43) Wu, L.; Xia, H.; Bai, J.; Xi, Y.; Wu, X.; Gao, L.; Qu, J.; Chen, Y. Diversified ring expansion of saturated cyclic amines enabled by azlactone insertion. *Nat. Chem.* **2024**, *16*, 1951−1959.
(44) Shimono, H.; Kusakabe, M.; Nagao, K.; Ohmiya, H. Carbonylative ring expansion of cyclic carboxylic acids. *J. Am. Chem. Soc.* **2025**, *147*, 45884−45892.
(45) Tan, T. D.; Zhou, F.; Quirion, K. P.; Wang, Y. Q.; Ng, D. Z. W.; Luo, X.; Chan, E. C. Y.; Liu, P.; Koh, M. J. Catalytic difluorocarbene insertion enables access to fluorinated oxetane isosteres. *Nat. Chem.* **2025**, *17*, 719−726.
(46) Zhou, X. Y.; Liu, L.; Lyu, H.; Wang, X. C. Modular alkyl growth in amines via the selective insertion of alkynes into C−C bonds. *Nat. Chem.* **2025**, *17*, 1323−1330.
(47) Nair, V.; Nair, S. M.; Mathai, S.; Liebscher, J.; Ziemer, B.; Narsimulu, K. The Rh(II) catalyzed reaction of diethyl diazomalonate with thietanes: a facile synthesis of tetrahydrothiophene derivatives via sulfonium ylides. *Tetrahedron Lett.* **2004**, *45*, 5759−5762.
(48) (a) Xie, J.; Zhao, W. Y.; Wang, J. Z.; Lyon, W. L.; Takanashi, N.; Long, A.; Sodano, T. M.; Kelly, C. B.; Bryan, M. C.; MacMillan, D. W. C. Couple-close: unified approach to semisaturated cyclic scaffolds. *Science* **2026**, *391*, 399−406. (b) Liu, Y.-P.; Guo, S.-Y.; Ding, Z.-Y.; Julaiti, Y.; Wang, L.-Y.; Wu, X.-F.; Chen, Q.-A. Pyridyl radical-induced catalytic reconstruction of cyclic sulfides. *ChemRxiv* **2026**, DOI: 10.26434/chemrxiv.10001578/v1.
(49) Kaiser, D.; Klose, I.; Oost, R.; Neuhaus, J.; Maulide, N. Bond-forming and -breaking reactions at sulfur(IV): sulfoxides, sulfonium salts, sulfur ylides, and sulfinate salts. *Chem. Rev.* **2019**, *119*, 8701−8780.
(50) Wang, G.; Han, D.; Li, Y.; Nie, Y.; Muthusamy, S.; Luo, Z.; Liu, B. Copper-mediated deconstructive ring cleavage of cyclic thioethers with boron compounds. *Org. Lett.* **2023**, *25*, 3522−3526.
(51) Humbrias-Martin, J.; Garrido-Gonzalez, J. J.; Medrano-Uribe, K.; Pelosi, G.; Laze, L.; Dell'Amico, L. Microfluidic photocatalytic ring expansion of sulfonium salts for the synthesis of cyclic sulfides. *ACS Catal.* **2025**, *15*, 6507−6513.
(52) Herk, L.; Feld, M.; Szwarc, M. Studies of "cage" reactions. *J. Am. Chem. Soc.* **1961**, *83*, 2998−3005.
(53) Braden, D. A.; Parrack, E. E.; Tyler, D. R. Solvent cage effects. I. Effect of radical mass and size on radical cage pair recombination efficiency. II. Is geminate recombination of polar radicals sensitive to solvent polarity? *Coord. Chem. Rev.* **2001**, *211*, 279−294.
(54) Lowry, M. S.; Goldsmith, J. I.; Slinker, J. D.; Rohl, R.; Pascal, R. A.; Malliaras, G. G.; Bernhard, S. Single-layer electroluminescent devices and photoinduced hydrogen production from an Ionic iridium(III) complex. *Chem. Mater.* **2005**, *17*, 5712−5719.
(55) Bryden, M. A.; Millward, F.; Lee, O. S.; Cork, L.; Gather, M. C.; Steffen, A.; Zysman-Colman, E. Lessons learnt in photocatalysis − the influence of solvent polarity and the photostability of the photocatalyst. *Chem. Sci.* **2024**, *15*, 3741−3757.
(56) Cui, W.; Li, X.; Guo, G.; Song, X.; Lv, J.; Yang, D. Radial type ring opening of sulfonium salts with dichalcogenides by visible light and copper catalysis. *Org. Lett.* **2022**, *24*, 5391−5396.
(57) Jin, J.; MacMillan, D. W. Direct α-arylation of ethers through the combination of photoredox-mediated C−H functionalization and the Minisci reaction. *Angew. Chem., Int. Ed.* **2015**, *54*, 1565−1569.
(58) Garza-Sanchez, R. A.; Tlahuext-Aca, A.; Tavakoli, G.; Glorius, F. Visible light-mediated direct decarboxylative C−H functionalization of heteroarenes. *ACS Catal.* **2017**, *7*, 4057−4061.
(59) Xu, L.; Shao, Z.; Wang, L.; Xiao, J. Tandem sp^3 C−H functionlization/decarboxylation of 2-alkylazaarenes with coumarin-3-carboxylic acids. *Org. Lett.* **2014**, *16*, 796−799.
(60) Niu, R.; Xiao, J.; Liang, T.; Li, X. Facile synthesis of azaarene-substituted 3-hydroxy-2-oxindoles via Brønsted acid catalyzed sp^3 C−H functionalization. *Org. Lett.* **2012**, *14*, 676−679.
(61) Drabowicz, J. Solid-phase silica-gel catalyzed α-halogenation of alkyl aryl sulfoxides with *N*-halosuccinimides. *Synthesis* **1986**, *1986*, 831−833.
(62) Hashmat Ali, M.; Hartman, M.; Lamp, K.; Schmitz, C.; Wencewicz, T. Oxidation of sulfides with *N*-bromosuccinimide in the presence of hydrated silica gel. *Synth. Commun.* **2006**, *36*, 1769−1777.
(63) Alfonzo, E.; Hande, S. M. Photoredox and weak Brønsted base dual catalysis: alkylation of α-thio alkyl radicals. *ACS Catal.* **2020**, *10*, 12590−12595.

https://doi.org/10.1021/jacs.6c09452
J. Am. Chem. Soc. XXXX, XXX, XXX−XXX